Case Report

Journal of Medical Research and Case Reports

eScientific

Hypothesis How Pressure May Affect the Healing Time of Hematomas

George C. Hartmann*

Strategy and Innovation Group, Xerox Corporate Research and Technology, Webster, NY, USA (retired)

***Corresponding Author:** George C. Hartmann, Strategy and Innovation Group, Xerox Corporate Research and Technology, Webster, NY, USA (retired).*

Abstract

This paper explores a hypothesis that considers the question how pressure may shorten the healing time of a hematoma or contusion. The purpose is to present a mathematical model for predictions based on the hypothesis that can be quantitatively compared to measurements. The time trajectory of the fluid volume in the hematoma is modeled by two rate equations, with rate parameters linked to healing and fluid transfer mechanisms. The flux of fluid leaving the hematoma pocket is assumed to be pressure dependent, consistent with Starling's principle, which asserts that the flux through a tissue layer is equal to the pressure gradient across the layer multiplied by the tissue hydraulic conductivity. Two contributions to the pressure are skin elasticity and applied compression. Shape measurements on two hematomas were made over the 10-week healing time. Model parameters are in fair agreement with values reported previously for wound contraction speed, tissue hydraulic conductivity, and skin elasticity.

Keywords: *Starling's principle; Pressure hypothesis; Hematoma; Healing time trajectory.*

Introduction

Hematomas (Hood [1] 2018) can occur in aesthetic surgery and implants of EP devices. To reduce pocket formation after pacemaker implants, specialized compression bandages (Valentino [2] 2015) can retard hematoma formation and speed up recovery.

In 2015 and 2020 the author who uses an anticoagulant, developed a hematoma on the forearm near the elbow after a fall, and later on the chest after an EP device was replaced. In both cases, the skin was not broken, but internal bleeding continued for several days forming a large hematoma. Measurements were made of major, minor and height axes until the wound healed after 10 weeks.

This paper investigates how pressure may shorten the healing time of a hematoma with a specific geometry, for example certain types of subcutaneous injuries and contusions. Two first-order rate equations describe the time-dependent geometry and rate of fluid removal through the floor of the hematoma pocket. Our initial hypothesis was that the fluid flux rate was constant throughout healing. Analysis of our data showed that the measured flux rate had a value close to previously measured rates for the mechanism of tissue hydraulic conductivity (Swabb [3] 1974). If so, the flux should be proportional to the pressure difference across the tissue layer at the pocket floor, and therefore implicitly depends on the pressure within the hematoma compartment. Coupled with studies that show compression bandages may aid healing, we are motivated to explore the effects of pressure on the healing trajectory.

Methods

Model Geometry

The volume of subdural hematomas was investigated by Gebel et al [4] (1998) who compared computer- assisted volumetric analysis of 44 subdural hematomas to a formula for the volume of an ellipsoid. They found a strong correlation. Taking the difference between two such shapes, Kasner [5] (1999) showed the formula can be extended to shell-like shapes. In this study, the hematoma shape is a raised dome under the skin and was represented by an ellipsoid which has been sliced in half called a triaxial semi-ellipsoid, similar in shape to a "shield cabochon" jewel. In this approximation, the volume is one-half that of an ellipsoid: the footprint is an ellipse and both cross-sections are semi-ellipses. All three axes may have different values. Geometric details are developed in Appendix A.

Wound Edge Healing

The footprint area decreases quadratically with time. This is shown in Appendix A, provided the edge of the wound advances toward the center according to a first-order rate equation,

$$\frac{dr(t)}{dt} = -\beta r(0) \quad \text{Eq. 1}$$

Eq. 1 is consistent with wound contraction (Romo [6] 2008) during the proliferation phase of wound healing in the band surrounding the footprint. The position of the wound edge is $r(t)$, $\beta r(0)$ is the wound edge-healing speed, and β is the wound contraction healing rate.

The measured wound edge-healing speed for our hematomas was 0.47 mm/day, somewhat less than surgical wounds with measured values of 0.75 mm/day for humans (Romo [6]) and 0.70 mm/day for pigs (Sharpe [7] 2013, data analyzed by the author).

Fluid Removal

Hematoma plasma fluid consists mostly of water, which moves across many biological membranes throughout the body by absorption in response to pressure and concentration gradients. For modeling, we propose that hematoma fluids are removed by absorption through the tissue in the footprint beneath the hematoma. The volume of fluid removed per unit time is proportional to the surface area of the footprint multiplied by the absorption parameter,

$$\frac{dV(t)}{dt} = -\alpha(t)S(t). \quad \text{Eq. 2}$$

$V(t)$ is the volume and $S(t)$ the footprint area of the hematoma (Appendix A). The absorption parameter $\alpha(t)$ is the flux of fluid (volume per second per unit area) moving to interstitial space beneath the footprint. Eq. 2 conforms with Darcy's law, or more generally Starling's principle, to be discussed at the end of the next section.

Constant Flux Assumption (Case 1)

Before considering the influence of pressure, in this section we examine a special case where the flux is assumed to be time-independent, identified as Case 1. This is the simplest assumption we can make, and it is useful in order to understand the associated implications. However, it will turn out in some situations to be inconsistent with Starling's principle as we will discuss at the end of this section. To examine this case, we set $\alpha(t)=\alpha_0$, a constant, in Eq. 2. Use Eq. 9 (Appendix A) for the time dependence of the surface area, change variables using $x=\beta t$, and define normalized height $f(x)=h(x)/h_0$ and normalized volume V/V_0 (the denominator is defined by Eq. 10, Appendix A). The dimensionless time parameter is limited to the range $0 < x < 1$, because the wound is closed when $x = 1$. The range is further restricted as we will see in a moment.

$$\frac{d}{dx}[(1-x)(1-gx)f(x)] = -3\lambda_0(1-x)(1-gx), \quad \text{Eq. 3}$$
$$\lambda_0 = \alpha_0/2\beta h_0$$

The parameter λ_0 is proportional to the magnitude of the flux. It is also equal to the ratio of two times: the wound edge closure time $1/\beta$, and $2h_0/\alpha_0$ related to the time required to empty the pocket. These two events are coincident if $\lambda_0 = 1$.

From Eq. 3 one finds,

$$V(x)/V_0 = 1 - 3\lambda_0 x + \frac{3(1+g)}{2}\lambda_0 x^2 - g\lambda_0 x^3$$

The time required for the volume to decrease to zero is given by the solution to $V(x_{root}) = 0$. The time range is therefore limited to $0 < x < x_{root}$. The root of the resulting cubic equation is algebraically cumbersome; however, both the volume and root expressions simplify if the parameter $g = 1$ (meaning the footprint is circular rather than elliptical),

$$V(x)/V_0 = 1 - \lambda_0 + \lambda_0 (1 - x)^2$$

$$V(x_0) = 0$$

$$x_0 = 1 - \sqrt[3]{|1 - 1/\lambda_0|}, \ \lambda_0 > 1 \text{ and } g = 1$$

The volume decreases to zero when $x = x_0$. Physically, the flux is large enough to empty the pocket before $x = 1$, when the footprint has closed. The time range of our problem is limited to $0 < x < x_0$.

If $\lambda_0 < 1$, the flux rate is too small to remove all the fluid before the footprint closes, and fluid remains trapped. If this happens, the geometry of the current model may not be applicable, so we restrict our attention to situations where $\lambda_0 > 1$.

The solution of Eq. 3 for the normalized height $f(x) = h(x)/h_0$ is

$$f(x) = \frac{1 - \lambda_0 x \left[3 - \left(\frac{3}{2}\right)(1+g)x + gx^2\right]}{(1-x)(1-gx)}, \ x < x_{root} \text{ and } \lambda_0 > 1$$

This simplifies if g=1

$$f(x) = \frac{1 - \lambda_0}{(1-x)^2} + \lambda_0(1-x), \ x < x_0 \text{ and } \lambda_0 > 1$$

This simplifies further if $\lambda_0 = 1$ to $x_0 = 1$, and $f(x) = 1-x$.

The cubic $V(x)/V_0$ was fitted by regression to measurements of hematoma volume versus time. A preliminary result is that the fitted value of λ_0 is very close to 1.0. Knowing that, one can estimate the value of the flux parameter α_0. The value is similar to benchtop measurements of flux for steady-state flow of plasma fluid through discs of subcutaneous tissue (Swabb [3]). Swabb found a linear relationship between flux and pressure gradient across the tissue layer in accordance with Darcy's law (devised in 1856 for soil mechanics). This law has been extensively studied for many types of tissue, and is comprehensively reviewed by Levick [8] (1987).

If absorption follows Darcy's law, or more generally Starling's principle (Matthay [9] 2006) from 1896 and later revisions (Michel [10] 1997) the flux through the hematoma floor depends on the pocket pressure minus the interstitial pressure. If the pocket pressure should vary with time, the flux will also vary with time, in conflict with our Case 1 assumption that the flux is constant.

Pressure Model

Our hypothesis is that the fluid flux across the tissue at the floor of the pocket is enhanced by additional pressure from external compression and skin elasticity. Interactions of this kind have been studied in connection with rabbit joints (Knight [11] 1985) - referred to as a "non-linear pressure-flow relationship". It is beyond our scope to speculate on the physiology, except to suggest linkage to Starling's principle, which asserts that the flux is proportional to the pressure difference across the floor tissue. On both sides of the floor, there are hydrostatic and osmotic pressure components. We are focused on the slowly-varying situation lasting many weeks, where the net pressure difference moves fluid from the pocket to interstitial space in accordance with Starling's principle.

An important application of Starling's principle describes fluid flow to and from a capillary bed, with subtle interplay between hydrostatic and osmotic pressures. The capillary hydrostatic pressure (CHP) (Boron [12] 2015) decreases from about 35 to 15 mm-Hg (above atmospheric pressure) as blood moves from the arteriole to venous ends of a capillary bed. The blood colloidal osmotic pressure (BCOP, about 28 mm-Hg) arises from a higher concentration of plasma proteins inside the capillary, so water is attracted to the capillary interior toward the venous end.

Similar mechanisms may occur with a hematoma. The pressure difference across the floor tissue that occurs naturally is denoted $DP_{net} = P_{pocket} - P_{interstitial}$. We now add two additional pressures to the pocket term, namely the applied pressure and elastic pressure due to skin stretching. The last two terms are "excess-pressure" above atmospheric pressure, indicated by the symbol Δ. This modifies the flux,

$$\alpha(t) = \frac{C}{\delta Y}\left[DP_{net} + \Delta P_{applied} + \Delta P_{elastic}\right]. \quad \text{Eq. 4}$$

Here C is the hydraulic conductivity and δY is the thickness of the tissue layer beneath the pocket floor. If the last two terms are absent, this reduces to the usual form of Darcy's law. Since most of fluid is leaving the cavity during the 10-week recovery period, we ignore short-time transients that may occur over the first few days and assume DP_{net} reaches a steady-state value. Eq. 4 means that the flux increases if the pressure increases, which will shorten the time required to empty the pocket.

The elastic pressure depends on the elastic properties of skin. Investigations of pressure in balloons and hollow viscera has a venerable history including Faraday (1824) who invented the rubber balloon, Osborne [13] (1909) and DePascalis [14] (2018) who extended the analysis to include non-linear viscoelastic thick-walled shells. We follow Osborne's model, which expressed the excess pressure (the difference of pressure inside and outside) in terms of viscera radius and elasticity. Osborne assumed a Hookian dependence of tension on strain described by Hooke's constant (1678). An expression for the pressure based on Osborne's model is proposed by Eq. 11, Appendix B.

$$\Delta P_{elastic}(t) = \frac{4Kh(t)}{r_a(t)^2} \qquad \text{Eq. 5}$$

where K is Hooke's elastic constant for skin, h(t) is the cavity height and r_a is the footprint radius.

Eq. 3 for Case 1 shows that the parameter g has a modest effect on height and volume, and so at this point, we assume g = 1, which simplifies the footprint shape from ellipse to circle. After substituting Eq. 4 (modified flux) and Eq. 9 (surface area) into Eq. 2, and expressing the result using dimensionless parameters, the pressure model becomes,

$$\frac{d}{dx}[(1-x)^2 f(x)] = -3\lambda_A(1-x)^2 - 3\lambda_B f(x), \quad \text{Eq. 6}$$

$$\lambda_A = (DP_{net} + \Delta P_{applied})/P_{scale}$$

$$\lambda_B = \Delta P_{elastic}(0)/P_{scale}$$

$$P_{scale} = 2\beta h_0\, \delta Y/C$$

$$\Delta P_{elastic}(x) = \Delta P_{elastic}(0) \frac{f(x)}{(1-x)^2}$$

$$\Delta P_{elastic}(0) = 4Kh_0/r_a^2(0)$$

$$DP_{net} = \lambda_0\, P_{scale}$$

$$\frac{DP_{net} + \Delta P_{applied} + \Delta P_{elastic}(x)}{P_{scale}} = \lambda_A + \lambda_B \frac{f(x)}{(1-x)^2}$$

The factor dividing the pressure terms is identified as P_{scale}, a unit of pressure. Using Swabb's measurements of hydraulic conductivity (for Darcy's Law) that relates flux to pressure gradient, our measured values of flux correspond to a pressure gradient of about 40 mm-Hg/cm. Assuming the thickness of the tissue layer on the floor of the hematoma is $\delta Y \approx 0.1$ cm, the inferred pressure drop across

the floor is $DP_{net} \approx 4$ mm-Hg. Since $\lambda_0 \approx 1$, we estimate $P_{scale} \approx 4$ mm-Hg.

Case 1 is included in Eq. 6 as a special case when $\Delta P_{applied} = 0$ and $\Delta P_{elastic} = 0$, so that $\lambda_B \to 0$ and $\lambda_A \to \lambda_0$.

Elastic Pressure Unrealistically Large (Assumption for Case 2)

In this sub-section, we examine a second situation that yields a straightforward analytic solution for the elastic pressure. We imagine the elastic pressure term to be much larger than the constant pressure term, including DP_{net}, which we temporarily neglect by setting $\lambda_A = 0$. Eq. 6 becomes (with solution),

$$\frac{d}{dx}[(1-x)^2 f(x)] = -3\lambda_B f(x), \quad \text{Eq. 7}$$

$$f(x) = \frac{exp\left[-\frac{3\lambda_B x}{1-x}\right]}{(1-x)^2}$$

$$\Delta P_{elastic}(x)/\Delta P_{elastic}(0) = \frac{exp\left[-\frac{3\lambda_B x}{1-x}\right]}{(1-x)^4}$$

$$V(x)/V_0 = exp\left[-\frac{3\lambda_B x}{1-x}\right]$$

The elastic pressure depends on the parameter λ_B, related to the elastic properties of skin.

If the strain is less than about 0.4, the stress-strain relationship is linear (Daly [15] 1979). The values of Young's modulus E range widely depending on skin location on the body, persons age (Pawlaczyk [16] 2013) and type of test. Values range from about E =37 to 1050 mm-Hg (Kalra [17] 2016). Young's modulus is related to Hooke's constant and depends on the membrane thickness as outlined in Appendix B. With E=37 mm-Hg, and skin thickness of 1 mm, Hooke's constant can be estimated, and from Eq. 6 the initial elastic pressure is about (0.8 to 8) mm-Hg. Considering the wide range for Young's modulus just cited, much larger values are possible, and so the contribution of the skin-elasticity pressure may range from negligible for some persons to significant for others.

Pressure Model Predictions

Eq. 6 quantifies how the combination of applied pressure and elastic pressure may shorten recovery. It can be rearranged and written (with solution),

$$\frac{df(x)}{dx} + \frac{3\lambda_B - 2(1-x)}{(1-x)^2} f(x) + 3\,\lambda_A = 0 \quad \text{Eq. 8}$$

$$f(x) = \frac{9\lambda_A\lambda_B^2}{2(1-x)} + \frac{3\lambda_A\lambda_B}{2} + \lambda_A(1-x) + \frac{exp\left(-\frac{3\lambda_B}{1-x}\right)}{(1-x)^2}\left[\Lambda - \frac{27\lambda_A\lambda_B^3}{2} Ei\left(\frac{3\lambda_B}{1-x}\right)\right]$$

$$\Lambda = exp(3\lambda_B)\left[1 - \lambda_A\left(1 + \frac{3}{2}\lambda_B + \frac{9}{2}\lambda_B^2\right)\right] + \frac{27}{2}\lambda_A\lambda_B^3 Ei(3\lambda_B)$$

The solution (Wolfram [18] 2020) includes the exponential integral Ei(z); it was numerically evaluated using a power series with 24 terms, with accuracy of a few percent provided z ≤ 15. The constant of integration was determined by the condition f(0) = 1. The total excess pressure (the sum of the pressure across the footprint tissue, applied pressure and elastic pressure) is found by substituting f(x) into the last line of Eq. 6. The solutions for Cases 1 and 2 are recovered if (λ_A, λ_B) are equal to (1,0) and (0,1), respectively.

Results and Discussion

Volume trajectories predicted by Eq. 8 were compared to geometric measurements for two healing hematomas (Figure 1); the parameters (λ_A, λ_B) defined in Eq. 6 were estimated by chi-squared minimization. The resulting values provide the best fit of the full model to the data for each hematoma. The parameter values (Table 1) can be interpreted as follows. The hematoma located on the forearm near elbow had a small footprint and a high dome that stretched the skin, consequently elastic pressure was large (with a best fit value of λ_B = 1.02) compared to the smaller constant pressure term (λ_A = 0.15). The other hematoma, located on chest, was the opposite, with a large footprint but shallow dome which did not stretch the skin, so the elastic pressure parameter was small (λ_B = 0.0) and the constant pressure parameter was comparatively large (λ_A = 1.0) .

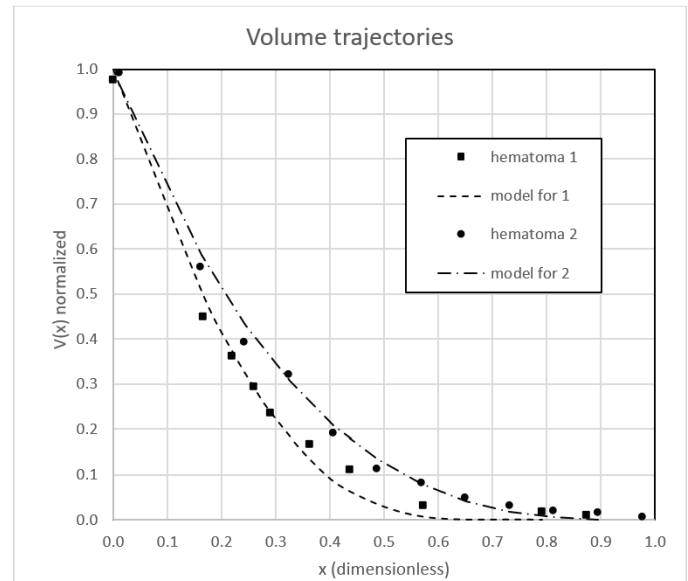|	Hematoma 1	Hematoma 2
h_0	1.4 cm	0.97 cm
S_0	17 cm^2	120 cm^2
V_0	16 cm^3	78 cm^3
g	0.63	0.66
λ_A (constant pressure)	0.15	1.0
λ_B (elastic pressure)	1.02	0.0
β/day	0.0104	0.0116

Table 1

Figure 1: *Model compared to measured volume trajectories. Adjustable parameters λ_A and λ_B were determined by chi-squared minimization with values listed in Table 1.*

Predictions from Eq. 8 are shown in Figures 2 and 3, which provides two views of the time evolution, namely, hematoma thickness in Figure 2 and total volume in Figure 3. For the full pressure model, the starting pressure when x=0 is $\lambda_A + \lambda_B$ (normalized units). The time coordinate ranges between 0 and a value given by f (x_0) = 0, corresponding to zero volume (this range limitation was described earlier for Case 1). The value of x_0 was estimated using Eq. 8 by a numerical computation - the curves in Figure 3 stop at this value, at which point the pressure is λ_A.

Predictions were calculated for two initial values of the total pressure (1.0 and 1.3). Figures 2 and 3 illustrate what occurs if the initial total pressure is assumed to be distributed in three different ways between constant pressure (100%, 50%, 0%) and elastic pressure (0%, 50%, 100%). This results in six pairs of values of (λ_A, λ_B). Figure 2 shows how increasing the initial total pressure causes the hematoma thickness to decrease to zero in a shorter time. If the initial total pressure is equal to 1 pressure unit, the thickness decreases to zero in about 1 dimensionless time-unit. If this pressure is shared between constant and elastic components, according to 50:50% and 0:100% the thickness decreases to zero in about 0.6 to 0.7 time-units. One reason why the time to empty is shortened is that the elastic pressure increases slightly as shown in Figure 3 owing to the assumption that the edge healing speed is

a constant. The time to empty is further shortened to the range of about 0.4 to 0.6 time-units if the total initial pressure is increased from 1.0 to 1.3.
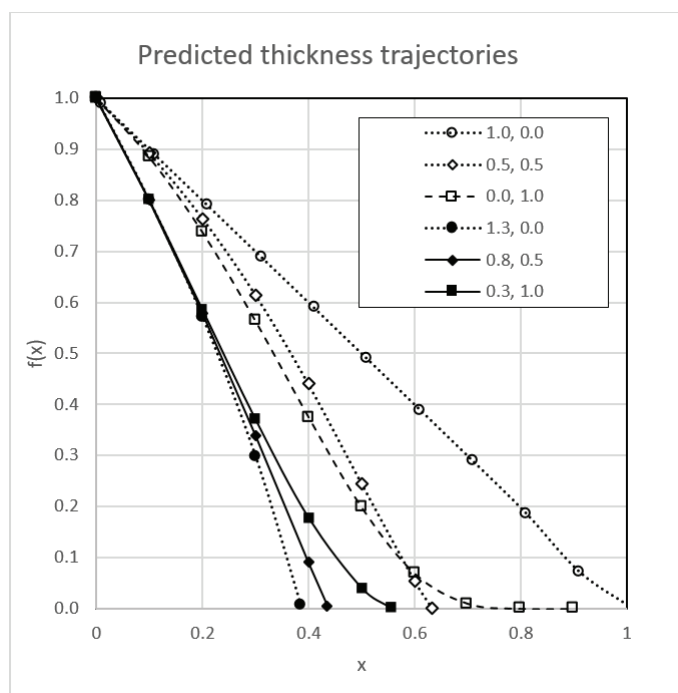
Figure 2: Predicted (normalized) thickness trajectories (the two numbers in the legend are λ_A, λ_B).

A limitation of this pressure model arises from our assumption that the wound edge-healing rate is independent of pressure. This presumes that the healing wound edge advances at the same speed regardless of the pressure that may develop within the hematoma pocket, which is an over-simplification. As edge healing shrinks the wound footprint, this model can force the total pressure to exceed an (unknown) threshold value, causing the footprint to abruptly enlarge by tearing the edge. Information about the strength of the wound edge is needed to anticipate discontinuous events like this. In this paper's treatment of the hypothesis, unreasonably large values of pressure can occur with certain combinations of the values of (λ_A, λ_B). The values chosen for Figures 2 and 3 avoid this condition.

These examples suggest how elastic pressure and compression pressure can decrease the healing time. The flux increases with pressure, which shortens the time required to empty the pocket.
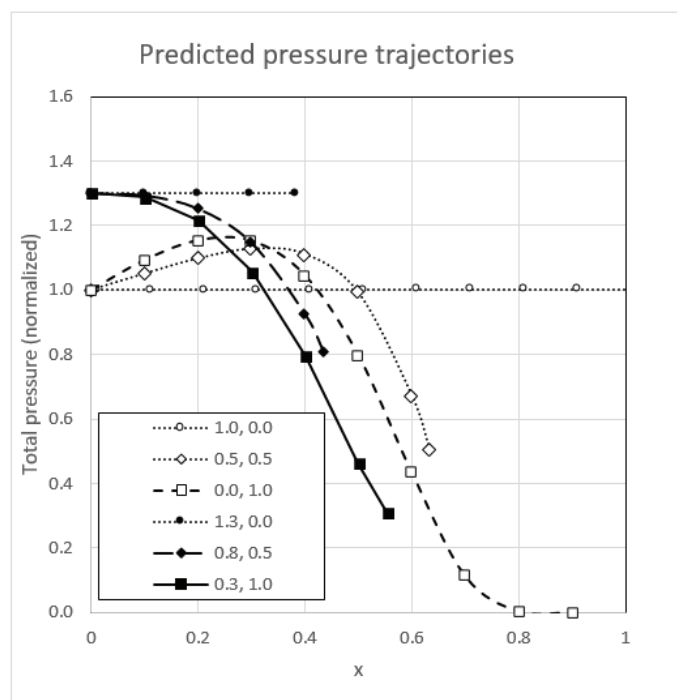
Figure 3: Predicted (normalized) pressure trajectories (the two numbers in the legend are λ_A, λ_B). Curves are labeled in the same order as Figure 2.

Conclusion

The purpose of this paper was to present a mathematical model of our hypothesis to enable predictions that can be quantitatively compared to measurements. The hypothesis presumes fluid is removed from the floor of a hematoma by absorption following Darcy's law or more generally, Starling's principle. These laws imply that the flux should depend on the incremental pressure inside the hematoma pocket arising from compression and elastic skin stretching. The resulting time-dependence of the model is surprisingly complex, and demonstrates that careful measurements will be required to confirm all the predicted features. Apart from geometric parameters, the model depends on just three physiological parameters: β (wound contraction rate), C (tissue hydraulic conductivity) and K (Hooke's constant for skin).

The model offers a way to estimate healing time reduction enabled by external compression. Evidence of the proposed mechanism could be explored by experiments on similar types of hematomas using a tonometer to track the pressure trajectory. Such observations might confirm the hypothesis, and enable refinement of the model assumptions.

Appendix A. Geometry

This Appendix uses the solution of Eq. 1 to find the time-dependence of the major and minor axes of the semi-ellipsoid that represents the hematoma shape. The solution of Eq. 1 for the minor axis is

$$r_a(t) = r_a(0)[1-\beta t] , \quad 0 < \beta t < 1$$

where the edge-healing speed is $\beta r_a(0)$. This expression applies until $\beta t \rightarrow 1$ and the wound is closed. If the major axis heals with the same speed, we find

$$r_b(t) = r_a(t) + [r_b(0) - r_a(0)] = r_b(0)[1 - g\beta t] ,$$

where $g = r_a(0)/r_b(0)$. As the surface area shrinks, the ratio of minor to major axes changes, until just before closure the wound is narrow and long, like a button hole. If $g = 1$, the footprint shape simplifies from ellipse to circle. The footprint area decreases quadratically with time,

$$S(t) = \pi r_a(t) r_b(t) = S_0 (1 - \beta t)(1 - g\beta t). \quad \text{Eq. 9}$$

where $S_0 = \pi r_a(0) r_b(0)$. The volume of the semi-ellipsoid is

$$V(t) = \frac{2\pi}{3} r_a(t) r_b(t) h(t) = V_0(1 - \beta t)(1 - g\beta t)\frac{h(t)}{h_0}, \quad \text{Eq. 10}$$

where the initial value of the volume is $V_o = \frac{2\pi}{3} r_a(0) r_b(0) h_0$.

Appendix B. Pressure Inside Hollow Viscera

Appendix B presents a parametric model for the elastic pressure as a function of the elastic parameters of skin and skin strain for the hematoma geometry. Following Osborne [13], the hematoma surface is represented by a section of a sphere formed by an elastic material obeying Hooke's law. When the pocket forms, the skin is stretched to form a shallow dome, raised an amount h above the surrounding skin surface. The dome is envisioned as the cap of a balloon with radius R restrained by the edge of a rigid circular hole (the hematoma footprint) with radius r. Osborne shows that the balloon pressure (excess above external atmospheric pressure) is related to the radius and tension by $\Delta P = 2T/R$. Before the skin is stretched, the tension is zero and so $\Delta P = 0$. After the skin is stretched, from geometry the balloon radius is $R = (r^2+h^2)/2h \cong r^2/2h$. The tension is proportional to Hooke's constant K times the fractional stretching of the skin denoted $\Delta L/L$, equal to the amount the dome arc length has stretched divided by the footprint diameter. Consequently $\Delta P \cong 4K(h/r^2)\Delta L/L$. Expressions for the fractional stretching can be derived and depending on the geometric assumptions, and may introduce

additional dependence on h and r. Knowing that $0 < h < h_0$, we propose a simple linear interpolation between 0 and h_0 to represent the pressure due to skin stretching,

$$\Delta P_{elastic} \cong 4K \frac{h}{r^2} \quad \text{Eq. 11}$$

Support for the parametric dependence proposed by Eq. 11 can be found from the bulge test (Chen [19] 2015), a measurement technique used to determine the material properties of thin films of materials including polymers, where pressure is applied to one side of a thin membrane of material covering a rigid hole with radius r, and the deformation h is measured as a function of applied pressure. For small deformations, the data is represented by Eq. 11, with measured pressure depending linearly on h and inversely on r^2.

Ghatak [20] (2013) derived a relation between the pressure and Young's modulus E for a balloon with thickness Z made of material that obeys Hooke's law. For small values of strain, comparing Ghatak's pressure expression with Osborne's (which depends on Hooke's constant K), we find K= 2EZ.

The author has no conflict of interest.

References

1. K. Hood, N. G. Kumar, C. Kaoutzanis. (2018). "Hematomas in Aesthetic Surgery", Aesthetic Surgery Journal 38, 9.
2. V. Valentino, Y. J. Greenberg, F. Yang. (2015). "A Unique Pressure Bandage Approach for the Prevention of Device Pocket Hematoma", EP Lab Digest 15, 6.
3. E. A. Swabb, J. Wei, P. M. Gullino. (1974). "Diffusion and Convection in Normal and Neoplastic Tissues", Cancer Research 34, 2814-2822.
4. J. M. Gebel, C. A. Sila, M. A. Sloan, C. B. Granger, J. P. Weisenberger, C. L. Green, E. J. Topol, K. W. Mahaffey. (1998). "Comparison of the ABC/2 Estimation Technique to Computer-Assisted Volumetric Analysis of Intraparenchymal and Subdural Hematomas Complicating the GUSTO-1 Trial", Stroke 29 (9) 1799-1801.

5. S. E. Kasner. (1999). "Geometry and Subdural Hematoma Volume", Stroke 30(1)188.

6. T. Romo, J. M. Pearson, H. Yalamanchili, R. A. Zoumalan. (2008). "Wound Healing, Skin", eMedicine Specialties, Wound Healing and Care.

7. J. R. Sharpe, Y. Martin. (2013). "Strategies Demonstrating Efficacy in Reducing Wound Contraction in vivo", Advances in Wound Care (New Rochelle), 2(4) 167-175.

8. J. R. Levick. (1987). "Review Article: Flow Through Interstitium and Other Fibrous Matrices", Quarterly Journal of Experimental Physiology, 72, 409-438.

9. M. A. Matthay, T. E. Quinn. (2006). "Starling Equation", Science Direct, Pulmonary Edema, Encyclopedia of Respiratory Medicine.

10. C. C. Michel. (1997). "Starling: The Formulation of his Hypothesis of Microvascular Fluid Exchange and its Significance after 100 Years", Experimental Physiology 82, 1-30.

11. D. Knight, J. R. Levick. (1985). "Effects of fluid pressure on the hydraulic conductance of interstitium and fenestrated endothelium in the rabbit knee", Journal of Physiology 360, 311-332.

12. W. F. Boron, Medical Physiology: A Cellular and Molecular Approach. Elsevier/Saunders, ISBN 978-1-4160-2328-9 (2005), numbers quoted by "Starling Equation", Wikipedia, https://en.wikipedia.org/wiki/Starling Equation.

13. W. A. Osborne, W. Sutherland. (1909). "The Elasticity of Rubber Balloons and Hollow Viscera", Proceedings of Royal Society of London, LXXXL, 485-499.

14. R. DePascalis, W. J. Parnell, I. D. Abrahams, T. Shearer, D. M. Daly, D. Grundy. (2018). "The inflation of viscoelastic balloons and hollow viscera", Proc. R. Soc. A 474.

15. C. H. Daly, G. F. Odland. (1979). "Age-related Changes in the Mechanical Properties of Human Skin", The Journal of Investigative Dermatology, 73 (1) 84-87.

16. M. Pawlaczyk, M. Lelonkiewicz, M. Wieczorowski. (2013). "Age-dependent biomechanical properties of the skin", Postepy Dermatol Alergol, 30 (5), 302-306.

17. Kalra, A. Lowe, A. M. Al-Jumaily. (2016). "Mechanical Behavior of Skin: A Review", J. Material Science and Engineering, 5 (4), 254.

18. Wolfram Alpha.com for ordinary differential equations. (2020).

19. K-S Chen, K-S Ou, "MEMS Residual Stress Characterization", Handbook of Silicon Based MEMS Materials and Technologies (2nd ed. 2015).

20. K. Ghatak. (2013). "Discussion neo-Hookian elasticity", Module 4: Non-linear elasticity, Lecture 25: Inflation of a balloon.